This document was prepared for the ETI by third parties under contract to the ETI. The ETI is making these documents and data available to the public to inform the debate on low carbon energy innovation and deployment.

Programme Area: Marine

Project: PerAWAT

Title: Design and Characterisation of Array Emulators

Abstract:

This report concerns the design of an array emulator to represent the rate of change of momentum due to energy extraction by an array of tidal stream turbines. An array emulator has been designed comprising a strip of identical circular discs of defined geometric porosity. Experiments are conducted with a multitude of discs to identify the variation of thrust coefficient on a single disc with geometric porosity. Thrust varies with geometric porosity, Reynolds number and blockage.

Context:

The Performance Assessment of Wave and Tidal Array Systems (PerAWaT) project, launched in October 2009 with £8m of ETI investment. The project delivered validated, commercial software tools capable of significantly reducing the levels of uncertainty associated with predicting the energy yield of major wave and tidal stream energy arrays. It also produced information that will help reduce commercial risk of future large scale wave and tidal array developments.

PerAWAT WG4 WP4 D2
Design and characterisation of array emulators

Project	PerAWAT
Work package	WG4
Deliverable	WG4 WP4 D2
Responsible author	Tim Stallard, Tong Feng
Second reading	Mat Thomson,
Circulation	UoM / GH
To be approved by	Robert Rawlinson-Smith (GH)
Date	30 May 2012
Issue	Version 2

Document revision history

Issue	Date	Summary
V1.0	28/05/2012	Version sent to GL-GH
V2.0	30/05/2012	Comments from M. Thomson GL-GH included

EXECUTIVE SUMMARY

The objective of this package of work is to improve understanding of the effects of energy extraction on the velocity and depth of flows at the basin scale. This is investigated via a series of experiments detailed in WG4WP4D1 for conduct at HR-Wallingford and comparison to shallow water simulations. This report concerns the design of an array emulator to represent the rate of change of momentum due to energy extraction by an array of tidal stream turbines. An array emulator has been designed comprising a strip of identical circular discs of defined geometric porosity. Experiments are conducted with a multitude of discs to identify the variation of thrust coefficient on a single disc with geometric porosity. Thrust varies with geometric porosity, Reynolds number and blockage. A porosity of 0.78 is selected for a set of discs of diameter D = 110 mm. The thrust coefficient and near-wake deficit of a strip of 14 discs at 1.2D centre-to-centre spacing are subsequently measured for strips of L=1.8 m only and 5.0 m within a wide channel of width W = 5.0 m and depth 0.2 m. Experiments are conducted for steady incident flows of speed 0.2 to 0.5 m/s. For L/W = 0.36, thrust coefficient is 0.73 and 1.1, when normalised to the rectangular area that encloses all discs and to disc area respectively. For L/W = 1.0, thrust coefficient increases with flow speed (0.35 – 0.5 m/s) with values in the range 0.86 – 0.90 (strip area) and 1.27 to 1.34 (disc area).

CONTENTS

1 INTRODUCTION

1.1 Scope of this document

This document constitutes the second deliverable (D2) of working group 4, work package 4 (WG4WP4) of the PerAWAT (Performance Assessment of Wave and Tidal Arrays) project funded by the Energy Technologies Institute (ETI). The project partners of this work package are Garrad Hassan (GH), Scott Draper (SD), University of Oxford (UoO) and the University of Manchester (UoM).

This work package addresses the impact of arrays on the global flow field through physical testing at a small geometric scale of the order of 1:300th scale. A specific objective is to obtain experimental data regarding the change of flow-speed and surface elevation at a regional, or basin, scale due to representative energy extraction. The focus of WG4WP4D1 is specification of a series of physical experiments to be conducted at the HR Wallingford Coastal Research Facility (CRF). Due to the small geometric scale of these experiments (water depth 200 mm) it is proposed that arrays, or lines, of rotors will be represented by a porous structure. This deliverable addresses the design and characterisation of a suitable 'array emulator'.

In this report, the design requirements for the array emulator are briefly reviewed (Section 2), an emulator design presented (Section 2.3) and a series of characterisation experiments summarised (Section 3). The design process includes a series of experiments regarding the variation of thrust coefficient of a disc with geometric porosity. A suitable porosity is subsequently identified and an array emulator comprising a line of porous discs is detailed. Variation of both thrust (drag) and velocity deficit are obtained by experiments in steady flow conducted at University of Manchester. An overview is given of the experimental process and main findings (Section 4).

1.2 Specific tasks associated with WG4 WP4

D1: Design and test specification

D2: Construction, testing and characterisation of array emulators
A brief report demonstrating that the array emulators are manufactured assembled and tested to specification. Characterisation detailed in the report.

D3: Construction, calibration, testing and reporting of coastal basin scale experiments.

Note: Much of the experimental work reported in this study was conducted in parallel with the specification report, WG4WP4D1. This report was originally scheduled for completion prior to both conduct of the experimental programme of D1 at HR-Wallingford (HRW) and preparation of the basin scale analysis report, WG4WP4D3. However, due to an opportunity to reduce the risk associated with the HRW schedule, the characterisation experiments conducted at University of Manchester and reported in Section 3 were completed after the HRW experiments.

1.3 Experimental Programme

The acceptance criteria as stated in the PerAWaT technology contract is as follows:

> "A brief report demonstrating that the array emulators are manufactured, assembled and tested to specification. Characterisation detailed in the report."

2 ARRAY EMULATOR DEVELOPMENT

2.1 Emulator Specification

The turbine array emulators are required for use in basin scale experiments at the CRF. The main parameters associated with these experiments are summarised in Table 2.1. Since energy extraction is equivalent to the rate of change of momentum the effect of turbines is described by a thrust (C_T) coefficient. Throughout this report, two thrust coefficients are reported:

C_T based on strip area = $F_x / ½\rho U_0^2 LD$

C_T based on disc area = $F_x / ½ \rho U_0^2 N¼\pi D^2$

where L and D the length and height of a fence comprising *N* discs of diameter *D*. The objective of this study is to develop an array emulator and characterise the variation of thrust coefficient over a representative range of flow speeds (0 to 0.5 m/s). To ensure that both the net thrust on each fence and the change of the velocity is measurable in the CRF experiments, a target thrust coefficient of approximately 1.0 based on disc was employed to inform design.

Table 2.1: Summary of geometry and flow-ranges for CRF basin scale experiments

	Channel	Headland
Speed range, U_0:	±0.5 m/s	±0.35 m/s
Water depth, h	0.2 m	
Channel width, W	9 m	7.5 – 9 m
Channel Re, hU_0/ν:	< 100k	< 70 k
Channel Fr, $U_0/(gh)^{1/2}$:	0.36	0.25
Fence height, D	0.11 m	
Fence length, L	1.8 m to 5.4 m	
Target thrust coefficient, $Fx/½\rho U_0^2 DL$	~0.8 on strip area	

Several options were considered for design of the array emulator ranging from multiple turbines through multiple porous discs to a constant porosity rectangular structure. At the small geometric scale (0.2 m depth, 0.11 m diameter) it is not practical to represent energy extraction by multiple small-scale rotors. This is due to the prohibitively low Reynolds number and relatively large mechanical friction. As such the workplan for WG4WP4 proposed a strip of porous, static structures. The options considered included:

A) A rectangular section of constant porosity mesh of height *D* and length *L*.
B) A line of circular porous discs of diameter *D* with end-end length *L*.

Preliminary experiments were conducted using a rectangular area of wire mesh. However, the necessarily high porosity of the mesh resulted in an unsatisfactorily low structural stiffness leading to low confidence in the thrust measurements. Furthermore, in order to characterise the variation of thrust coefficient with strip porosity it would have been necessary to manufacture and construct multiple strips. This was beyond the remit of the proposed programme of work. Instead, the approach taken has been to represent an array by a line of closely spaced circular porous discs. This approach has allowed characterisation of the variation of thrust coefficient with porosity of an individual disc, a brief investigation of the effect of channel Reynolds number and blockage and subsequent characterisation of the thrust coefficient on a strip of discs.

2.2 Porosity

Porous discs have been employed in numerous numerical studies and several experimental studies of tidal stream systems to represent the effect of energy extraction by a rotor. Assuming inviscid flow, Glauert showed that the resistance of a porous disc (here denoted k_n) can be related to the thrust

coefficient as $C_T = 1/(k_n+k_n/4)^2$. This resistance coefficient is not directly related to the geometry of the porous media. Geometric porosity is typically defined as the ratio of open area to solid (or closed) area $K = A_{0PEN} / A_{SOLID}$ such that the total area of the disc is $A = ¼\pi D^2 = A_{0PEN}(1+K)$.

There is limited published information concerning the variation of thrust coefficient with geometric porosity of either discs or strips. Myers (2011) tested individual porous discs of 100 mm diameter and porosity 0.35 to 0.48 and reported thrust coefficients in the range 0.61-0.94. Blunden et al. (2008) employ a 100 mm high porous fence to represent a row of aligned rotors. Porosity was selected such that the thrust coefficient on the fence is 'equal to that averaged over a row of turbines, with the same dimensions, each with a higher C_T and at an arbitrary spacing (e.g. $C_T = 0.8$ at 2D lateral spacing).' Fences constructed had a width of 0.95 m and height of 0.1 m simulating a row of 0.1 m D turbines at 2D spacing. Porosities of approximately 90% were employed.

Due to the limited information available to inform disc porosity, experiments were conducted with isolated discs to quantify the variation of thrust coefficient (C_T) with geometric porosity. These experiments were conducted using the flume, equipment and methods as detailed in WG4WP2D1-D5. Flow speed is $U_0 = 0.5$ m/s, water depth $h = 0.45$ m and disc diameter D=270 mm. Reynolds number of the flow is 200k approx. and blockage is approximately 2.5% (single disc area / channel area = $A_D/A_C = ¼\pi D^2/Wh$). Fifteen different discs were manufactured by drilling holes of uniform diameter d = 10 mm or 12 mm or 14 mm in 6 mm thick acrylic to produce porosities $0.2 < K < 1.6$. Measurements of thrust (Figure 2.1) demonstrate a nearly linear variation of thrust thrust coefficient with porosity over the range tested.

Further tests at a lower Reynolds number (Re ~ 70k) and higher blockage ($A_D/A_C = ¼\pi D^2/Wh$ ~ 25%) were also conducted with a smaller set of discs. These were conducted using the equipment and methods detailed in WG4WP2D1-5 but a smaller flume of 0.3 m width, flow speed $U_0 = 0.35$ m/s, water depth $h = 0.25$ m and disc diameter D = 150 mm. Discs comprise uniform diameter holes d = 10 – 14 mm drilled in 6 mm thick acrylic. Over the range $K < 0.9$, the effects of blockage and Reynolds number increase CT. These single-disc thrust measurements show

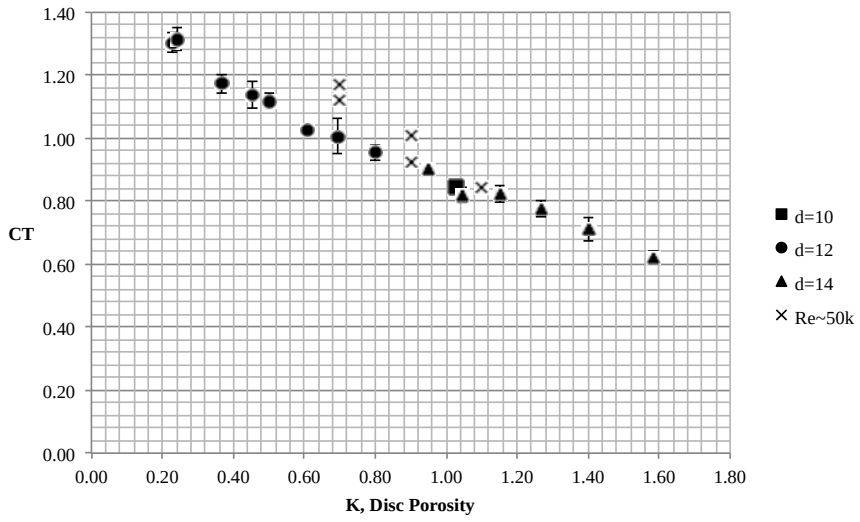

Figure 2.1: Variation of thrust coefficient with geometric porosity ($K = A_{OPEN} / A_{SOLID}$) for range of hole diameters (d). Data for Re ~ 225 k and range of hole diameters (solid markers) and Re ~ 50 k (x).

2.3 Emulator Design

The depth and array emulator height and flow velocity for the basin scale experiments are defined as Table 2.1. Target thrust coefficient based on strip area is $C_T = Fx/½rU_0^2A_S \sim 0.8$ where $A_S = LD$. To

relate this to the thrust coefficient on individual discs it is assumed that net force on the rectangular strip is equivalent to net force on the N discs that comprise the strip. i.e.:

$$C_{T,STRIP}\tfrac{1}{2}\rho U_0^2 LD = F_x = C_{T,DISC}\tfrac{1}{2}\rho U_0^2 N\tfrac{1}{4}\pi D^2$$

$$C_{T,STRIP}\tfrac{1}{2}\rho U_0^2 A_{STRIP} = F_x = C_{T,DISC}\tfrac{1}{2}\rho U_0^2 NA_{DISC}$$

Thus $C_{T,DISC} = C_{T,STRIP}A_{STRIP} / NA_{DISC}$

The number of discs N within a strip of length L is dependent on the centre-centre disc spacing s:

$$L = (N\text{-}1)Ds + D$$

Spacing also defines the inter-disc blockage (A_D/hsD). Thus to obtain a thrust coefficient of 0.8 based on strip area there are several possible combinations of spacing, disc number and disc thrust coefficient. Three possible options for attaining $C_{T,STRIP} \sim 0.8$ are summarised in Table 2.2:

Table 2.2: Estimated values of disc thrust coefficient and number required to generate $C_{T,STRIP} \sim 0.8$ from rectangular strip of height D = 0.11 m and L ~ 1.8 m.

Disc spacing s	Disc number N	Strip length L	Strip area LD	Disc area NAD	Disc Thrust CT	Disc Blockage A_D/hsD
1.1000	15.0000	1.804	0.1984	0.1425	1.1137	0.4
1.2000	**14.0000**	**1.826**	**0.2009**	**0.1330**	**1.2078**	**0.36**
1.3000	13.0000	1.826	0.2009	0.1235	1.3007	0.33

As disc-disc spacing is reduced the required disc number is increased and the blockage is increased. Since increase of C_T is observed as blockage is increased from 2.5% to 25% further increase is expected over the blockage range 25% to 40%. For spacing s = 1.1 and 1.3, thrust coefficients of 1.1 and 1.3 are required. Based on the data of Section 2.2 there is considerable uncertainty over which value of porosity would yield these thrust coefficients at high blockage. A spacing of s = 1.2 has been selected which corresponds to $C_T \sim 1.2$ based on disc area. Whilst there remains some uncertainty over the disc porosity that will develop this C_T value at blockage of 36%, this is within the range of porosities considered and some indicative estimates can be extrapolated. A disc of porosity $K \sim 0.75$ to 0.8 develops $C_T \sim 0.95$ at Re ~ 225 k and $A_D/A_C \sim 2.5\%$ and $C_T \sim 1.1$ at Re ~ 70 k and $A_D/A_C \sim 25\%$. For the higher blockage (>25 %) of the CRF fence experiments a thrust coefficient similar to 1.2 is expected.

2.4 Emulator Manufacture

Following the single disc porosity experiments and identification of porosity range $K = A_{OPEN} / A_{SOLID}$ = 0.75-0.8, a number of discs and support structure were manufactured for use in the CRF experiments. The equipment manufactured comprises:

- 42 individual discs of diameter D = 110 mm and hole diameter d = 12 mm with porosity K = 0.789 and geometry as shown in Appendix A Figure A.1. Manufactured from 6 mm thick acrylic.
- 42 No. vertical support rods 0.25 m long comprising M6 threaded rod with long hex nut clamped at lower end to mount each disc. (see Figure A.2)
- 3 No. Square Hollow Section (SHS) Aluminum 30x30 length 1760 (built in two parts for transport) with holes at 0.132 m centres to support 14 No. support rods and discs (see Figure A.2).

The arrangement of the disc and strip is given in Appendix A and illustrated in Figure 2.2.

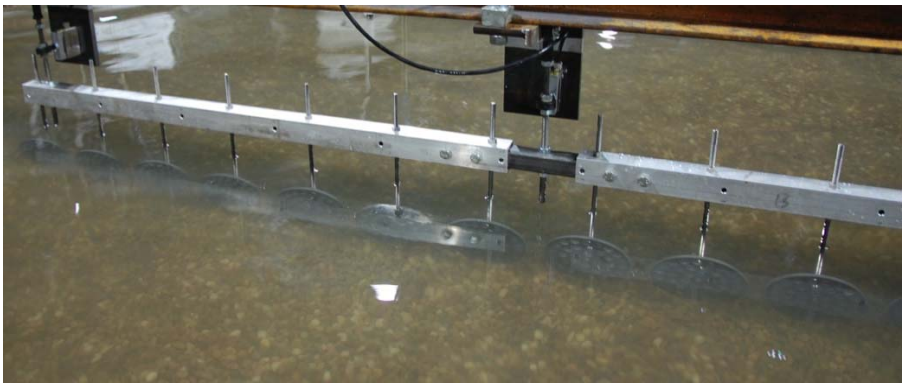

(a) 1.8 m long strip of 14 No. discs installed at HRW CRF. Ten discs shown indicating vertical support rod per disc and horizontal SHS located above waterline and supporting all discs.

(b) 3 No. sections of 1.8 m long strip of discs, total 42 discs, installed at HRW CRF. 3rd strip only part shown right hand side of image.

Figure 2.2: Strip of discs following manufacture at UoM and installation at HRW CRF.

3 ARRAY EMULATOR CHARACTERISATION

Experiments were conducted in the University of Manchester wide flume at a water depth of 0.2 m. The flume is 5 m wide and the test section is 12 m in length. Further description of the facility is given in WG4WP2D3-D5 with one notable difference: the porous weir described in WG4WP2D3 is not used since this was found to create a shallow wake that extended to the test section. For all tests the fence is located at X = 6 m measured from the inlet. A left-handed global co-ordinate system is used in which X is aligned with the direction of the flow, Y is horizontal across the width of the flume and Z is vertical (positive upwards). Data is presented in terms of absolute position relative to the origin of the flume in the Y-Z plane, (Y, Z) = (0, 0) located at the bottom left of the flume inlet and in terms of non-dimensional position relative to the centre of a rotor or fence in the stream-wise X-direction.

Data is collected for two fence configurations in water depth 200 mm:

A. 1.8 m strip only within 5 m wide channel.
B. 1.8 m strip within 5 m strip spanning full-width of 5 m wide channel

For both configurations the strip of discs comprises 14 No. discs of diameter D = 110 mm at 1.25D spanning 1.8 m (y=+/-0.9 m). For 2D modelling, the ratio of fence length (L) to flume width (W) is of relevance (L/W). For 3D modelling, the global blockage ratio is relevant (A/A_C) where A_C the vertical area of the channel. Two blockage ratios are defined with respect to the aggregate area of the discs ($N_{Disc}A_{Disc}$) and the area of the rectangular section containing the discs (LD).

Table 3.1: Geometry of disc and entire fence for both configurations. For both cases, force is only measured on the central 1.8 m section of the strip.

	1.8 m strip only (14 No. Discs)	Full-width
Number of discs, N_{Disc}	14	37
Disc diameter, D	0.11 m	
Disc area, A_{Disc}	0.0095 m^2	
Disc spacing, s	1.2D	
Disc Blockage, NA_{Disc}/A_C	0.133	0.35
Strip length, L	1.8 m	5.0 m
Strip Blockage, LD/A_C	0.20	0.55
2D Blockage, L/W	0.36	1.00

The following measurements were sampled at 200 Hz for 1 minute:

- U_0 Incident axial velocity across line of fence prior to fence installation U_0
- U_1 Upstream axial velocity (single point) at mid-depth
- F_x Horizontal Force, F_x
- $U_{nD}(Y)$ Downstream axial velocity traverse: multiple Y increments at X = nD

Steady incident velocities and location of downstream traverse summarised in Table 3.2.

Table 3.2: Location of downstream traverse for each configuration and incident flow velocity.

U0 (m/s)	1.8 m strip only (L/W = 0.36)	Full-width (L/W = 1.0)
0.20	2D	-
0.35	2D and 12D	2D and 12D
0.50	2D	2D

3.1 Thrust Measurement

A single strip of discs comprises 14 No. discs each supported from a horizontal beam located above waterline by a 6 mm diameter vertical threaded rod. The horizontal beam is of square section and supported at 1.75 m centres by 2 No. strain gauged support structures. Each strain-gauged structure is identical to the system described in WG4WP2D4 Section 4.1 and comprises a 15 mm outer diameter stainless steel tube with 1 mm (approx.) wall thickness. Strain gauges are surface mounted 800 mm above a horizontal rod that is clamped to the square section beam. Disc centreline to beam centreline is 125 mm. For this application, the lever-arm from disc centreline (hub height) to strain gauge is 925 mm. Two moments are measured (M_1 and M_2) and the net force on the strip ($F_{x,strip} = N_{Disc}F_{x,Disc}$) obtained as:

$$F_{x,strip} = (M_1 + M_2) / 0.925$$

Each strain gauge is calibrated prior to test by application of fixed increment masses and a linear relationship is obtained between applied moment and measured voltage (method as WG4WP2D4).

3.2 Flow Measurement

Velocity is recorded at mid-depth using a single NORTEK Vectrino+ ADV with the probe head mounted horizontally such that:

ADV x-axis aligned with flume X-axis.
ADV y-axis aligned with flume Z-axis.
ADV z-axis aligned with flume Y-axis.

The Vectrino+ is supported on an automated traverse table manufactured by HR Wallingford. This facilitates multi-point measurements in the vertical Y-Z plane. Further details on both the Vectrino+ and traverse table are given in PerAWaT WG4 WP2 D4. In this application the Vectrino+ measurement volume is located at mid-depth for all measurements and traverses are conducted in the Y-axis only. The traverse table is repositioned manually to pre-defined increments in the X-axis.

3.3 Incident Velocity

Experiments are conducted in 200 mm water depth. Mean velocity is a linear function of pump capacity. Across the width of the channel mean velocity varies by approx. 10% of the width-averaged value. Pump capacity is selected to obtain target mean velocities of 0.2 m/s, 0.35 m/s and 0.5 m/s at mid-depth when averaged across the width of the channel. Lateral variation of velocity is shown in Figure 3.1. Corresponding measured mean velocities are 0.204, 0.358 and 0.512 m/s

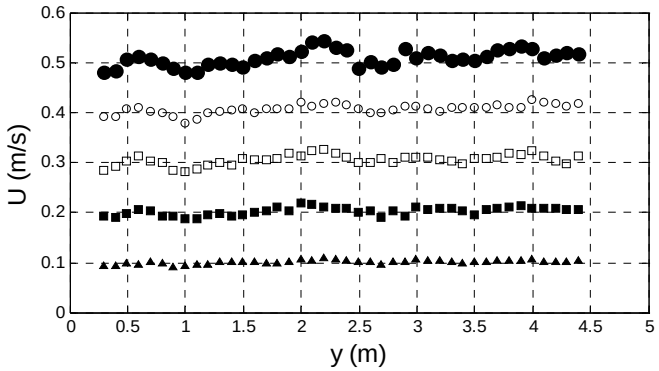

Figure 3.1: Variation of axial velocity with Y-ordinate along line of fence at X = 6D from inlet. Left side of flume at Y = 0, centreline of flume at Y=2.5 m. Data for range of pump capacities: 50% (solid circ), 40% (open circ), 30% (open square), 20% (solid square) and 10% (triangle).

3.4 Measured Thrust and Velocity Field, U_0 = 0.35 m/s

For each configuration listed in Table 4.1 1 min samples of all variables are recorded for 100 Y-axis locations of the downstream ADV over the range 470 < Y < 4470 mm. Relative to flume centreline at Y = 2500 mm. Thus, for each mean flow speed and configuration, the force reported is the average of 100 No. 1 min samples. The transverse variation of axial velocity is obtained at increments of dY = 50 mm for all configurations and increments of dY = 10 mm for one configuration. An example of the average of 1 min samples obtained for U_0 = 0.35 m/s and for both strip configurations is given in Figure 3.2.

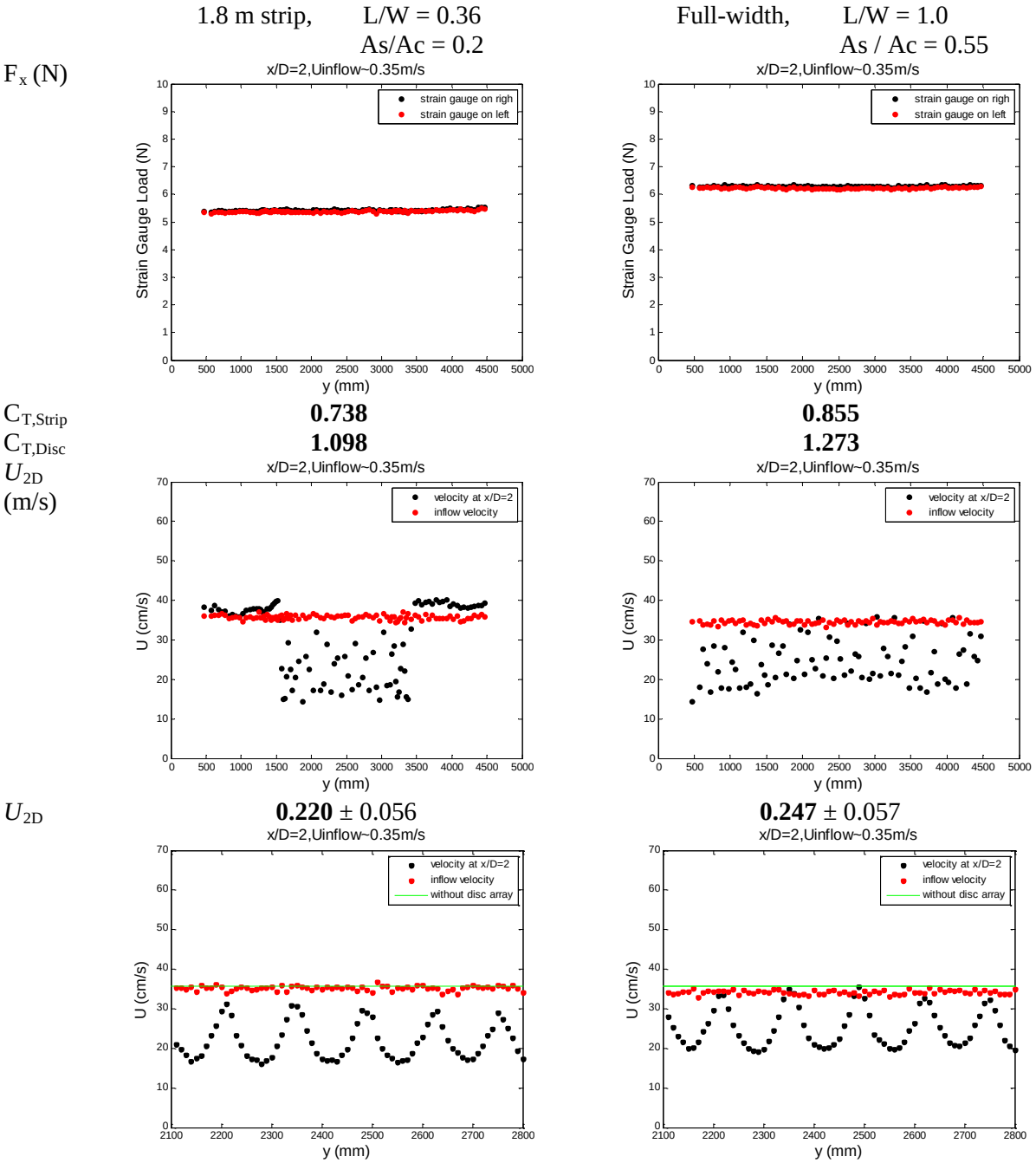

Figure 3.2: Thrust measurement (top) for each sample of velocity (mid) measured at 100 Y-ordinates at mid-depth at X=2D downstream. Incident U0 = 0.35 m/s. Detail of velocity also shown (btm).

Force:

For each 1 min sample, the mean force applied to each strain gauge differs by less than 2%. The variation of force across all 100 samples is also less than 2%.

Velocity:
Incident velocity (recorded by stationary ADV) does not vary substantially during the 100 minute test duration. Immediately downstream of the fence (X = 2D), velocity is reduced to a mean deficit of 40% and 30% for L/W = 0.36 and 1.0 respectively. Downstream of the strip there is significant variation of axial velocity between adjacent measurement increments (standard deviation ± 0.056 m/s and 0.057 m/s, Figure 3.2) as might be expected since dY = 50 mm is too coarse to resolve the structure of individual wakes. Measurements obtained at increments dY = 10 mm (btm frames Figure 3.2) over a small Y-range confirm that this variation is due to individual wakes. For both cases the flow is slightly asymmetric with lower wake velocity and lower bypass flow velocity observed at Y < 1000 mm than Y>4000. For L/W = 1.0, mean velocity is nearly constant across the channel (and strip) width. For L/W = 0.36 increased speed of the bypass flow is clearly observed (e.g. Y<1500, Y>3500).

Further downstream, individual wakes merge to a nearly uniform deficit by approximately 12D downstream (Figure 3.3). At this distance, deficit is 21% and 11% for L/W = 0.36 and 1.0 respectively. Increased speed of the bypass flow is evident for the part-width strip.

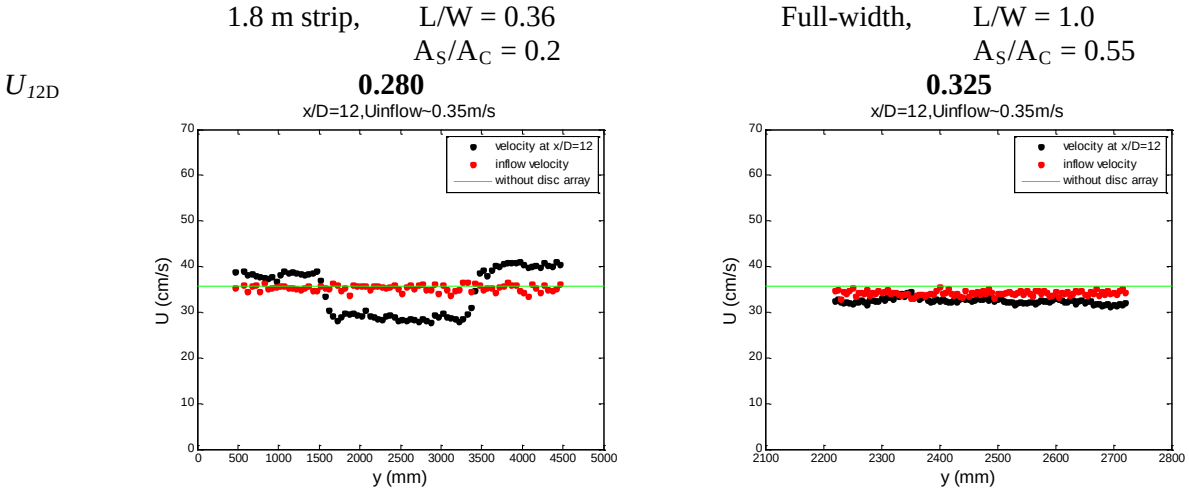

Figure 3.3: Axial velocity at mid-depth measured at multiple Y-increments at X = 12D downstream of strip of length L/W = 0.36 and 1.0.

3.5 Thrust Variation with Flow Speed

The data of Section 3.4 corresponds to an incident flow velocity of 0.35 m/s. Similar experiments were also conducted for 0.2 m/s and 0.5 m/s to quantify variation of thrust coefficient and velocity field changes with velocity. For this velocity range the Reynolds number range, is 40k – 100k based on channel depth (h=0.2 m), and 20k – 50k based on strip height (D = disc diameter). The Froude number is 0.15 to 0.7. Thrust coefficients, based on strip area and disc area, are shown in Figure 3.4.

For L/W = 0.36, there is negligible variation of thrust coefficient with velocity. However there is slightly greater variation of thrust over the 100 samples at the lowest speed tested. This is probably due to the small magnitude of the force measurements, of the order of 1.5 N per strain gauge. Thrust coefficient per disc is approximately 1.1 and thrust coefficient based on strip area is 0.73.

For L/W = 1.0, thrust coefficient increases with flow velocity. Thrust coefficient per disc increases from 1.27 at U = 0.35 m/s to 1.34 at U= 0.5m/s. Similarly the coefficient for the strip increases from 0.86 to 0.9.

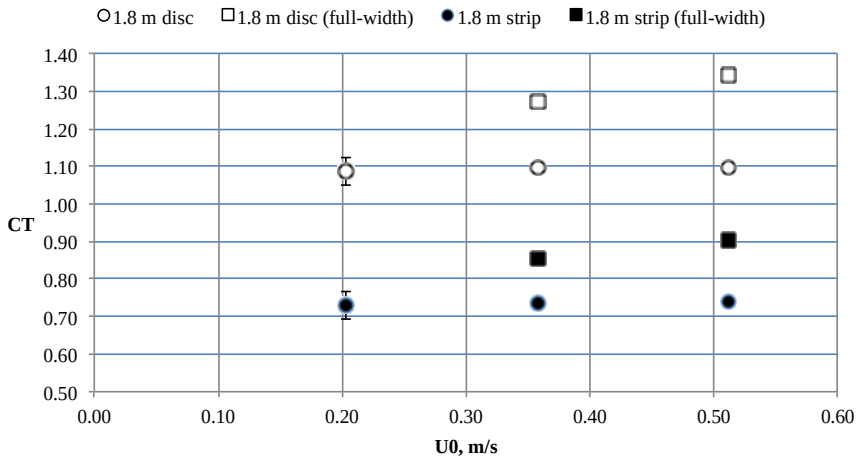

Figure 3.4: Variation of thrust coefficient normalised to strip area (solid) and to disc area (open) with flow-speed for: 1.8 m wide strip only (L/W = 0.36, As/Ac = 0.2, circle) and within 5 m strip spanning flume (L/W = 1, As / Ac = 0.55, square).

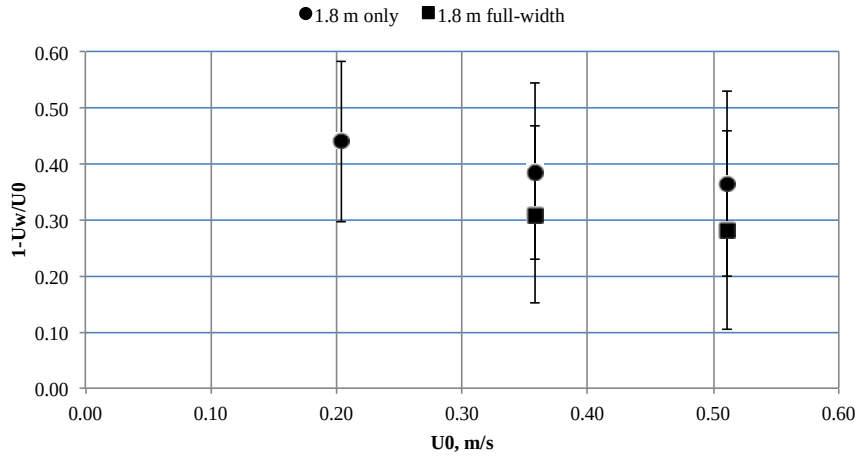

Figure 3.5: Variation of mean velocity deficit at X=2D downstream of strip across Y±0.75 m with flow-speed for: 1.8 m wide strip only (circle) and within 5 m strip spanning flume (square). Error bars indicate standard deviation of mean velocity across Y±0.75 m.

4 CONCLUSIONS

An array emulator comprising a strip of porous discs of diameter 110 mm has been developed and manufactured for use in the basin scale experiments at the HR-Wallingford Coastal Research Facility (CRF). Dimensions and flow-rates of the CRF experiments are defined in WG4WP4D1. The intention is to develop an array emulator with a target thrust coefficient, based on rectangular area of the strip, of approx. 0.8. Experiments are conducted that quantify the variation of thrust coefficient of a single porous disc with respect to geometric porosity. It is shown that disc thrust coefficient increases as channel Reynolds number is reduced and blockage ratio increased. These experiments inform selection of a disc porosity of 0.75 – 0.8. This is expected to develop a disc thrust coefficient of approx. 1.2 and hence strip thrust coefficient of 0.8.

Three identical support structures have been manufactured to support a total of 42 No. 110 mm diameter discs. Each array emulator represents a rectangular strip of width 1.8 m and height 0.11 m. Experiments have been conducted in steady flow at flow speeds of 0.2 m/s, 0.35 m/s and 0.5 m/s in the University of Manchester flume to characterise the thrust coefficient of the array emulator. Thrust coefficients are obtained for a strip length of part of the flume width (Length ~ 0.36 Width) and the full flume width (Length = Width). For the partly blocked case thrust coefficients are independent of flow speed with magnitude 0.78 based on rectangular strip area. For the fully blocked case, thrust coefficient increases with flow speed with magnitude 0.86 – 0.90. Three array emulators, each of 1.8 m length, have been manufactured and dispatched to HR-Wallingford. The array emulators have been installed at the Coastal Research Facility and experiments as described in WG4WP4D1 conducted.

REFERENCES

Daly, T., Myers, and Bahaj, A.S. Experimental analysis of the local flow effects around single row tidal turbine arrays. *Proc. 3rd International Conference on Ocean Energy*, Bilbao, 2010.

Draper, S. Physical Scale Modelling Specification, ETI PerAWaT Report WG4WP4D1 commissioned by GL-Garrad Hassan for ETI Project.

Myers, L.E. and Bahaj, A.S. An experimental investigation simulating flow effects in first generation marine current energy converter arrays. *Renewable Energy* 37 (2012) 28-36.

Stallard, T.J. Thomson, M., Collings, R., and Whelan, J, Calibration report for Scale Model Experiments. ETI PerAWAT WG4 WP2 D4, Feb 2011.

Thomson, M., Collings, R., Stallard, T. and Feng, T. Summary of findings from scale model study of an array of tidal stream rotors. ETI PerAWAT WG4 WP2 D5, Jun 2011.

APPENDIX 1: DISC AND STRIP ARRANGEMENT

Description of porous disc geometry and support structure for multiple porous discs.

porosity =
0.787
Holes =
37
OuterDiameter =
110 mm
HoleDiameter =
12 mm
Radius_Number_TopHoleDegrees =

45	19	0
30	12	0
15	6	0
0	0	0

CentreHoleDiameter =
4 mm

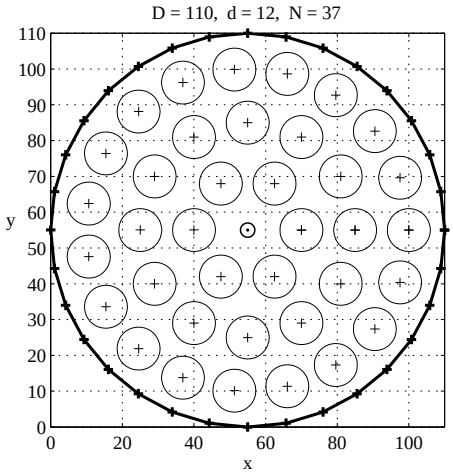

Figure A.1: Geometry of porous disc employed for Basin Scale experiments.

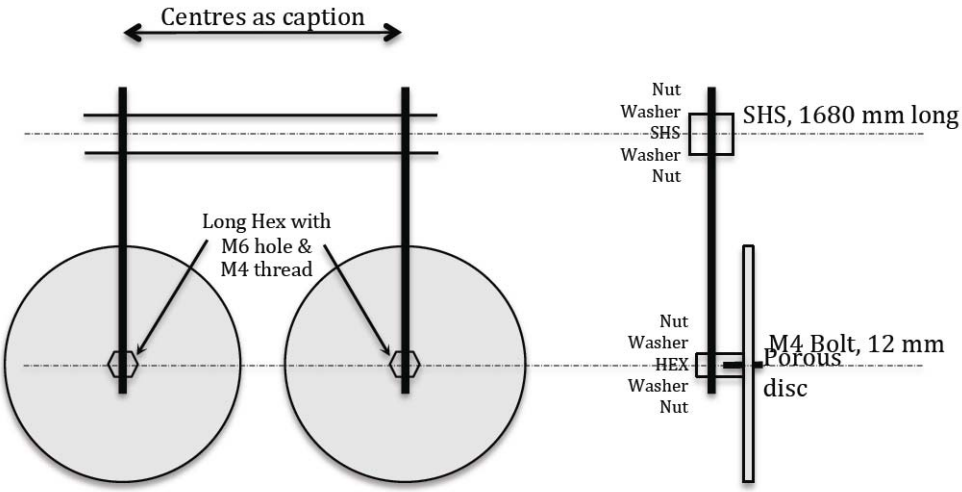

Figure A.2: Arrangement of support structure for multiple porous discs of diameter D = 110 mm and centres at $s = 1.2D$.